

# The pyCSAMT software package for enhancing the groundwater exploration technique using the CSAMT data

Kouao Laurent Kouadio<sup>\*1,3</sup>, Binbin Mi<sup>†1</sup>, Rong Liu<sup>‡1</sup>, Albert Okrah Malory<sup>§1</sup>, and Chunming Liu<sup>§2</sup>

<sup>1</sup> Key Laboratory of Geoscience Big Data and Deep Resource of Zhejiang Province, School of Earth Sciences, Zhejiang University, China. <sup>2</sup> Department of Geophysics, School of Geosciences and Info-physics, Central South University, China <sup>3</sup> Equipe de Recherche Géophysique Appliquée, Laboratoire de Géologie Ressources Minérales et Énergétiques, UFR des Sciences de la Terre et des Ressources Minières, Université Félix Houphouët-Boigny, Cote d'Ivoire ¶ Corresponding author

DOI: [10.xxxxxx/draft](https://doi.org/10.xxxxxx/draft)

## Software

- Review [↗](#)
- Repository [↗](#)
- Archive [↗](#)

Editor: [↗](#)

Submitted: 14 April 2022

Published: unpublished

## License

Authors of papers retain copyright and release the work under a Creative Commons Attribution 4.0 International License ([CC BY 4.0](#)).

## Summary

Controlled source audio-frequency magnetotelluric (CSAMT) is a frequency-domain electromagnetic method established as a good resistivity exploration tool for mapping the fault zones for groundwater exploration ([Asch & Sweetkind, 2011](#); [G. Bernard et al., 1997](#); [J. Bernard & Vachette, 1990](#); [Chouteau & Giroux, 2008](#); [Kouadio et al., 2020](#); [Liu et al., 2020](#)). However, the detection of fracture zone requires additional geophysical methods to supplement the CSAMT ([Guo et al., 2019](#); [Wadi, 2017](#); [Zonge & Hughes, 1991](#)). This is expensive and despite this combination, the misinterpretation of inversion results leads to unsuccessful drillings due to the wrong location of the boreholes ([Kouadio et al., 2020](#)). We, therefore, design the pyCSAMT software to solve this problem. First, the software used the geological data and previous borehole/well data collected in the survey area to predict the strata log at each station (pseudostratigraphic (PS)log). This allows to demarcate well the fracture zones. Secondly, it estimates the layer thicknesses with less margin error useful before the drilling operations. To test the efficiency of the software, the real CSAMT data, geological and boreholes data collected from the survey carried out in the Xingning area, Hunan province, China ([Kouadio et al., 2021](#)) were used. Additional to the examples scripts and workshop material, the results published in ([Kouadio et al., 2022](#)) validated the use of the software. Finally, the error thickness evaluated between the predicted log and the mechanical boreholes (borehole used for the test) was satisfactory with error less than 06 meters.

## Statement of need

pyCSAMT follows the modular approach of existing software like MTPy ([Krieger & Peacock, 2014](#)) and GMT ([Wessel & Smith, 1998](#)), and contains an inner handler to calibrate and to scale the raw data from different hardware into the appropriate units (SI). It recomputes the deviation errors before analysis and processing ([Mykle, 1996](#)). The software also includes some electromagnetic array profiling filters such as the trimming moving average, the fixed dipole-length moving average, and the adaptive-moving-average filter based on the idea of ([Torres-verdin & Bostick, 1992](#)) to correct the CSAMT data corrupted by the static shift effect ([Raymond, 1993](#); [Sanders et al., 1996, 2006](#)). Furthermore, the toolbox reads different CSAMT raw data formats (e.g., \*.AVG format ([Mykle, 1996](#); [Sanders et al., 2006](#)) from Zonge

\*Co-first author

†Co-first author

‡Co-first author

§Co-first author

Engineering), \*.DAT format proposed by (Chave & Smith, 1994) and the standard Electronic Data Interchange (EDI) file format). It is composed of three main packages with different roles: *ff*, *geodrill*, and *viewer*. The *ff* package encompasses the *core* and the *processing* (a set of *analysis* and *processing* modules) sub-packages. Overall, the packages provide features coded in Python classes, methods, and functions. Figure 1 shows an overview of pyCSAMT packages and sub-packages with their roles.

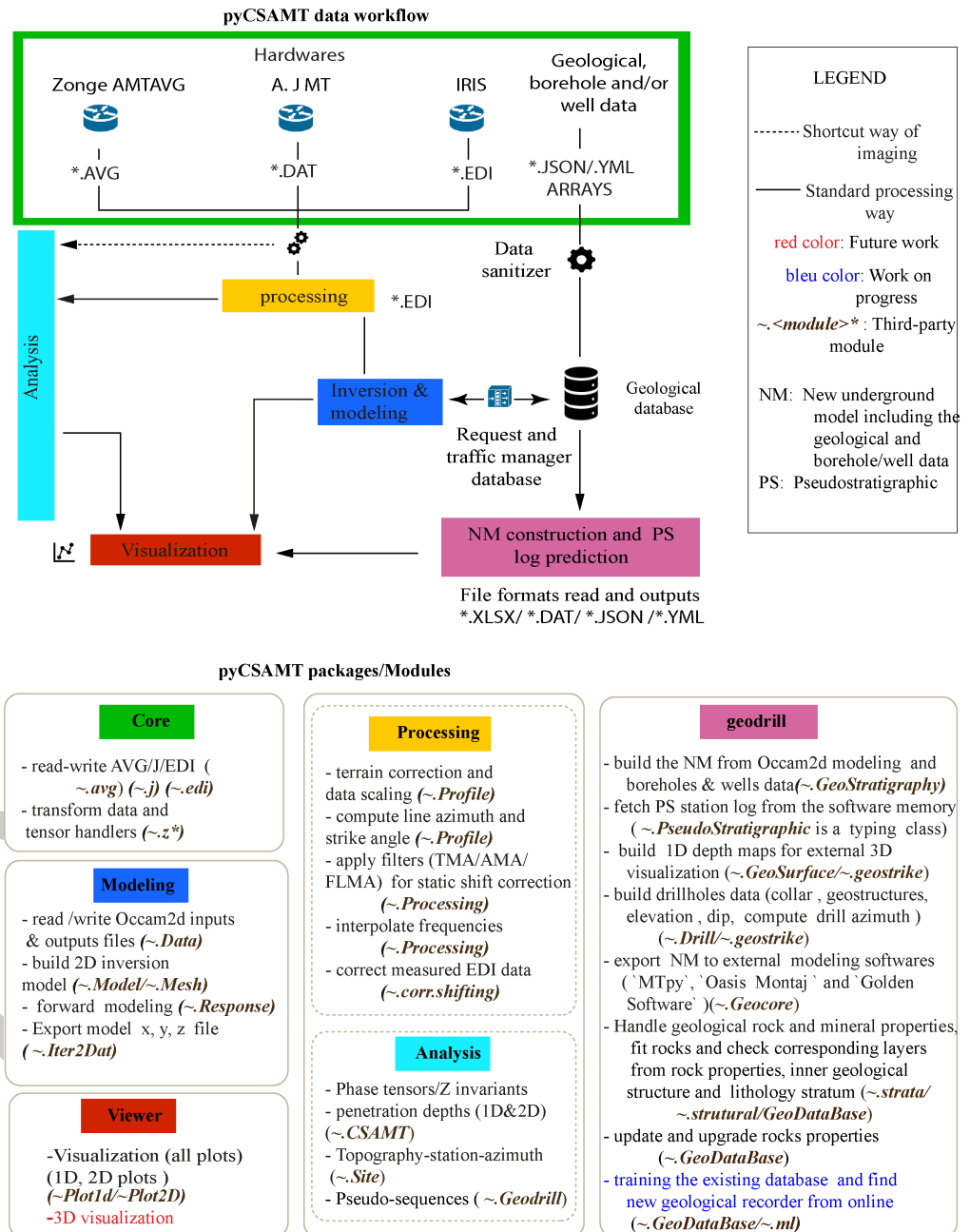


**Figure 1:** pyCSAMT packages structures and the keys modules. The colors in the workflow diagram represent which parts of the software are used in each step. For example, the modules in the geodrill packages are used for NM construction and PS prediction

The core sub-package contains functionality to read and write CSAMT data from industry-

standard formats such as \*.DAT, \*.AVG and \*.EDI including metadata from the header of the EDI file, the location, and also the impedance tensor (Z). The processing sub-package is designed to facilitate working with DAT, AVG and EDI data and generating inputs for existing third-party processing codes(e.g., the module Z of (Kirkby et al., 2019; Krieger & Peacock, 2014)). The viewer package is essentially dedicated to data and log sequences visualization (1D and 2D plots). The modeling package of the toolbox uses the finite-element (FE) structured grid and deals with the OCCAM2D software (DeGroot-Hedlin & Constable, 1990) to invert the processed data. It uses the FE algorithm developed by (Wannamaker et al., 1987) to generate the OCCAM2D input and output data for the forward model visualization. Moreover, it also provides some output files for other external modeling software like oasis montaj of Geosoft (GeosoftCorporation, 2021), and surfer of Golden Software corporations (GoldenSoftware, 2021). The geodrill package mainly deals with geological, borehole/well data collected from the survey area. It also includes a geological database composed of rock properties such as the electrical properties and the minerals classification of (Slichter & Telkes, 1942) and (Palacky, 1988) for new model (NM) construction (also called the geostratigraphy model). Moreover, an error map named *MisfitG* is computed between the the forward model and the NM to ascertain the underground layers misclassification. Furthermore, the PS technique developed in (Kouadio et al., 2022) is used for PS log prediction and thickness estimation. Indeed, the NM parameters are saved to the software memory from which the PS log under each station is retrieved.

## Acknowledgments

We thank the Subsurface Imaging and Sensing Laboratory of the School of Earth Sciences of Zhejiang University and Central South University for supervising the project. The development of this Python toolbox has been supported by the Key Laboratory of Geoscience Big Data and Deep Resource of Zhejiang Province of School of Earth Sciences at the National Zhejiang University, China.

## References

- Asch, T. H., & Sweetkind, D. S. (2011). Case History Audiomagnetotelluric characterization of range-front faults, Snake Range, Nevada. *Geophysics*, 76(1), 1–7.
- Bernard, G., Michel, C., Marc, D., & Michel, R. (1997). Use of the magnetotelluric method in the study of the deep Maestrichtian aquifer in Senegal. *Journal of Applied Geophysics*, 38(2), 77–96. [https://doi.org/10.1016/S0926-9851\(97\)00016-5](https://doi.org/10.1016/S0926-9851(97)00016-5)
- Bernard, J., & Vachette, C. (1990). Deep groundwater survey with audio-magnetotelluric soundings. *Annual Meeting Abstracts, Society of Exploration Geophysicists*, 2, 528–531.
- Chave, A. D., & Smith, J. T. (1994). On electric and magnetic galvanic distortion tensor decompositions. *Journal of Geophysical Research*, 99, 4669–4682. <https://doi.org/10.1029/93JB03368>
- Chouteau, M., & Giroux, B. (2008). Michel chouteau bernard giroux ´. In *G´eophysique appliqu´ee II: Methodes electriques* (p. 76).
- DeGroot-Hedlin, C., & Constable, S. (1990). Occam's inversion to generate smooth, two-dimensional models from magnetotelluric data. *Geophysics*, 55(12), 1613–1624.
- GeosoftCorporation. (2021). Geosoft | Oasis montaj - Seequent. In *Geosoft* (p. 1). <https://www.seequent.com/products-solutions/geosoft-oasis-montaj/>
- GoldenSoftware. (2021). Surfer® | 2D & 3D mapping,modeling & analysis software for scientists and engineers. In *goldensoftware.com* (p. 1). <https://www.goldensoftware.com/products/surfer>

- 91 Guo, Z., Hu, L., Liu, C., Cao, C., & Liu, J. (2019). Application of the CSAMT method to Pb–Zn  
92 Mineral. *Minerals*, 9(726), 2–12. <https://doi.org/https://doi.org/10.3390/min9120726>
- 93 Kirkby, A., Zhang, F., Peacock, J., Hassan, R., & Duan, J. (2019). The MTPy software  
94 package for magnetotelluric data analysis and visualisation. *Journal of Open Source*  
95 *Software*, 4(37), 1358. <https://doi.org/10.21105/joss.01358>
- 96 Kouadio, K. L., Liu, R., Mi, B., & Liu, C. (2022). pyCSAMT: An alternative Python toolbox for  
97 groundwater exploration using controlled source audio-frequency magnetotelluric. *Journal*  
98 *of Applied Geophysics*, 104, 104647. <https://doi.org/https://doi.org/10.1016/j.jappgeo.2022.104647>
- 100 Kouadio, K. L., Rong, L., Malory, A. O., Liu, C., & Xia, J. (2021). *CSAMT data in*  
101 *Xingning area, Hunan Province, China* [Data set]. Zenodo. <https://doi.org/https://doi.org/10.5281/zenodo.5533467>
- 103 Kouadio, K. L., Xu, Y., Liu, C., & Boukhalfa, Z. (2020). Two-dimensional inversion of  
104 CSAMT data and three-dimensional geological mapping for groundwater exploration in  
105 Tongkeng Area, Hunan Province, China. *Journal of Applied Geophysics*, 183, 104204.  
106 <https://doi.org/10.1016/j.jappgeo.2020.104204>
- 107 Krieger, L., & Peacock, J. R. (2014). MTPy: A Python toolbox for magnetotellurics. *Computers*  
108 *and Geosciences*, 72, 167–175. <https://doi.org/10.1016/j.cageo.2014.07.013>
- 109 Liu, R., Liu, J., Wang, J., Liu, Z., & Guo, R. (2020). A time-lapse CSEM monitoring study  
110 for hydraulic fracturing in shale gas reservoir A time-lapse CSEM monitoring study for  
111 hydraulic fracturing in shale gas reservoir. *Marine and Petroleum Geology*, 120(December),  
112 104545. <https://doi.org/10.1016/j.marpetgeo.2020.104545>
- 113 Mykle, R. (1996). AMTAVG documentation: CSAMT data averaging program. In *Zonge*  
114 *Engineering & Research Organization, Inc* (p. 48). [http://www.zonge.com/legacy/PDF\\_](http://www.zonge.com/legacy/PDF_DatPro/AmtAvg.pdf)  
115 [DatPro/AmtAvg.pdf](http://www.zonge.com/legacy/PDF_DatPro/AmtAvg.pdf)
- 116 Palacky, G. J. (1988). Resistivity Characteristics of Geologic Targets. *Geophysics*, 3, 52–129.  
117 <https://doi.org/10.1190/1.9781560802631.ch3>
- 118 Raymond, M. (1993). Documentation Zonge Data Processing TEM Data Averaging Program.  
119 *Imaging*, 10(520), 1–39.
- 120 Sanders, B., Raymond, M., & Rykala, J. (1996). SHRED Documentation ZONGE Data Pro-  
121 cessing GDP Data Reformat Program. In *Zonge Engineering & Research Organization, Inc.*  
122 (p. 39).
- 123 Sanders, B., Raymond, M., & Rykala, J. (2006). ASTATIC Documentation. In *Zonge*  
124 *Engineering & Research Organization, Inc* (pp. 1–23). [http://www.zonge.com/legacy/](http://www.zonge.com/legacy/PDF_DatPro/Astatic.pdf)  
125 [PDF\\_DatPro/Astatic.pdf](http://www.zonge.com/legacy/PDF_DatPro/Astatic.pdf)
- 126 Slichter, L. B., & Telkes, M. (1942). *Electrical Properties of Rocks and Minerals* (F. B. C.  
127 Spicer, J. F. Schairer, & S. H. Cecil, Eds.; Geological). © 1942 Geological Society of  
128 America. <https://doi.org/https://doi.org/10.1130/SPE36-p299>
- 129 Torres-verdín, C., & Bostick, F. X. (1992). Principles of spatial surface electric field filtering in  
130 magnetotellurics: Electromagnetic array profiling ( EMAP ). *Geophysics*, 57(4), 25–34.  
131 <https://doi.org/10.1190/1.2400625>
- 132 Wadi, A. (2017). *Comparison of Dipole-Dipole IP/ Resistivity and CSAMT Results*.
- 133 Wannamaker, P. E., Stodt, J. A., & Rijo, L. (1987). A stable finite element solution for  
134 two-dimensional magnetotelluric modelling Stodt Rijo. *Geophysics*, 88, 277–296.
- 135 Wessel, D. E., & Smith, W. H. (1998). New, improved version of generic mapping tools  
136 released. *Eos Trans. Am. Geophys. Union*, 79, 579.

- <sup>137</sup> Zonge, L., & Hughes, L. J. (1991). Controlled Source Audio-Frequency Magnetotellurics.  
<sup>138</sup> *Society of Exploration Geophysicists*, 2, 713–809.

DRAFT